## RESEARCH ARTICLE



# Real-time influence of intracellular acidification and Na<sup>+</sup>/H<sup>+</sup> exchanger inhibition on in-cell pyruvate metabolism in the perfused mouse heart: A <sup>31</sup>P-NMR and hyperpolarized <sup>13</sup>C-**NMR** study

David Shaul 1,2 | Naama Lev-Cohain 1 | Gal Sapir 1,2 0 | Jacob Sosna 1 | 

#### Correspondence

Rachel Katz-Brull, Department of Radiology, Hadassah Medical Organization and Faculty of Medicine, Hebrew University of Jerusalem, Jerusalem, Israel,

Email: rkb@hadassah.org.il

#### Funding information

H2020 Future and Emerging Technologies, Grant/Award Number: 858149-AlternativesToGd: Israel Science Foundation, Grant/Award Number: 1379/18; Ministry of Science and Technology, Israel, Grant/Award Number: 3-15892

## Abstract

Disruption of acid-base balance is linked to various diseases and conditions. In the heart, intracellular acidification is associated with heart failure, maladaptive cardiac hypertrophy, and myocardial ischemia. Previously, we have reported that the ratio of the in-cell lactate dehydrogenase (LDH) to pyruvate dehydrogenase (PDH) activities is correlated with cardiac pH. To further characterize the basis for this correlation, these in-cell activities were investigated under induced intracellular acidification without and with Na<sup>+</sup>/H<sup>+</sup> exchanger (NHE1) inhibition by zoniporide. Male mouse hearts (n = 30) were isolated and perfused retrogradely. Intracellular acidification was performed in two ways: (1) with the NH<sub>4</sub>Cl prepulse methodology; and (2) by combining the NH<sub>4</sub>Cl prepulse with zoniporide. <sup>31</sup>P NMR spectroscopy was used to determine the intracellular cardiac pH and to quantify the adenosine triphosphate and phosphocreatine content. Hyperpolarized [1-13C]pyruvate was obtained using dissolution dynamic nuclear polarization. <sup>13</sup>C NMR spectroscopy was used to monitor hyperpolarized [1-13C]pyruvate metabolism and determine enzyme activities in real time at a temporal resolution of a few seconds using the product-selective saturating excitation approach. The intracellular acidification induced by the NH<sub>4</sub>Cl prepulse led to reduced LDH and PDH activities (-16% and -39%, respectively). This finding is in line with previous evidence of reduced myocardial contraction and therefore reduced metabolic activity upon intracellular acidification. Concomitantly, the LDH/PDH activity ratio increased with the reduction in pH, as previously reported. Combining the NH<sub>4</sub>Cl prepulse with zoniporide led to a greater reduction in LDH activity (-29%) and to increased PDH activity (+40%). These changes resulted in a surprising decrease in the LDH/PDH ratio, as opposed to previous

Abbreviations: AAR, area at risk; ADP, adenosine diphosphate; AON, area of necrosis; AOP, area of perfused myocardium; ATP, adenosine triphosphate; CBE, CI-/HCO<sub>3</sub>- exchanger; CHE, CI^/OH^ exchanger; dDNP, dissolution dynamic nuclear polarization; DO, dissolved oxygen; EVB, Evan's blue; Ini, injection; KH buffer, Krebs-Henseleit buffer; LDH, lactate dehydrogenase; MR, magnetic resonance; NAD+, nicotinamide adenine dinucleotide (oxidized); NADH, nicotinamide adenine dinucleotide (reduced); NBC, Na+/HCO<sub>3</sub>- co-transporter; NHE, Na+/H+ exchanger; PCr, phosphocreatine; PDH, pyruvate dehydrogenase; pHi, intracellular pH; Pin, intracellular inorganic phosphate; TTC, triphenyltetrazolium chloride.

This is an open access article under the terms of the Creative Commons Attribution-NonCommercial-NoDerivs License, which permits use and distribution in any medium, provided the original work is properly cited, the use is non-commercial and no modifications or adaptations are made. © 2023 The Authors. NMR in Biomedicine published by John Wiley & Sons Ltd.

<sup>&</sup>lt;sup>1</sup>Department of Radiology, Hadassah Medical Organization and Faculty of Medicine, Hebrew University of Jerusalem, Jerusalem, Israel

<sup>&</sup>lt;sup>2</sup>The Wohl Institute for Translational Medicine, Hadassah Medical Organization, Jerusalem, Israel

<sup>&</sup>lt;sup>3</sup>School of Computer Science and Engineering, The Hebrew University of Jerusalem, Jerusalem, Israel

predictions. Zoniporide alone (without intracellular acidification) did not change these enzyme activities. A possible explanation for the enzymatic changes observed during the combination of the NH<sub>4</sub>Cl prepulse and NHE1 inhibition may be related to mitochondrial NHE1 inhibition, which likely negates the mitochondrial matrix acidification. This effect, combined with the increased acidity in the cytosol, would result in an enhanced H<sup>+</sup> gradient across the mitochondrial membrane and a temporarily higher pyruvate transport into the mitochondria, thereby increasing the PDH activity at the expense of the cytosolic LDH activity. These findings demonstrate the complexity of in-cell cardiac metabolism and its dependence on intracellular acidification. This study demonstrates the capabilities and limitations of hyperpolarized [1- $^{13}$ C] pyruvate in the characterization of intracellular acidification as regards cardiac pathologies.

#### KEYWORDS

ammonium chloride, intracellular pH, lactate dehydrogenase, mitochondrial pH, NHE1, pyruvate dehydrogenase, zoniporide

## 1 | INTRODUCTION

Intracellular pH (pH<sub>i</sub>) plays an important role in the regulation of cellular enzymatic activity<sup>1</sup> and protein stability.<sup>2</sup> In the heart, it has a profound effect on contractile function, calcium homeostasis, and electrical activity.<sup>3-5</sup> Hyperpolarized magnetic resonance using the dissolution dynamic nuclear polarization (dDNP) approach is useful in determining intracellular enzymatic activity in a noninvasive and nonradioactive manner. This technology has previously enabled multiple studies of in-cell metabolic reactions determined in vivo, in real time, in preclinical models,<sup>6-12</sup> and in men.<sup>13,14</sup> Multiple studies have also shown such in-cell enzyme activities in perfused whole organs from rodents such as heart and liver,<sup>15,16</sup> tissue slices,<sup>17-22</sup> and organoids.<sup>23</sup> In the dDNP approach, the magnetic resonance signal of the metabolic substrate can be increased by several orders of magnitude,<sup>24</sup> enabling observation of its metabolic fates in real time, as long as those occur before the meta-stable hyperpolarized state has decayed (a few minutes).

Hyperpolarized [1-<sup>13</sup>C]pyruvate is the dominant metabolic substrate in dDNP-hyperpolarized magnetic resonance (MR) studies because of its superb polarization properties, and the central role pyruvate metabolism plays in cellular energetics, at the crossroads of aerobic and anaerobic metabolism. Hyperpolarized [1-<sup>13</sup>C]pyruvate was useful in the characterization of several conditions in the heart, in preclinical animal models, such as heart failure, sichemia, sichemia, reperfusion injury, myocardial infarction, and cardiac hypertrophy. Of note, hyperpolarized [1-<sup>13</sup>C]pyruvate is approved for testing in humans and has shown utility in clinical cardiac studies. 13,14

Pyruvate metabolism may be affected by pH<sub>i</sub>, as two of its major fates, the conversion to acetyl-CoA and CO<sub>2</sub> by pyruvate dehydrogenase (PDH) and the conversion to lactate by lactate dehydrogenase (LDH), have both been shown, in vitro, to be pH dependent<sup>26,27</sup>; a pH drop in the physiological range increased the activity of LDH<sup>26</sup> and decreased the activity of PDH.<sup>27</sup>

As the hyperpolarized MR approach enables monitoring of in-cell enzymatic activities without tissue homogenizations or compartmentalization, it offers the possibility to test the effects of pH<sub>i</sub> on these enzyme activities in-cell, in the viable organ. However, we note that a study of the effect of pH<sub>i</sub> in the whole heart on these in-cell enzyme activities is complicated, because of the difference in the cellular compartments in which these enzymes reside. While LDH is a cytosolic enzyme, PDH is a mitochondrial enzyme. Because pH<sub>i</sub> may be distributed unevenly among the cellular compartments, it is not straightforward to both control and predict the effect of pH<sub>i</sub> on these cellular enzymes. In addition, we note that in the intact cell, pH<sub>i</sub> changes will always affect a broad variety of intracellular enzymes, and these may involve opposing systems that are activated or inhibited at the same time.<sup>28</sup> Such changes may have indirect effects on LDH and PDH activities. Previously, we have reported that the in-cell LDH to PDH activities ratio in the perfused mouse heart is strongly correlated with cardiac pH.<sup>29</sup> Here, we aimed at further characterizing the mechanism underlying this observation and its possible utility as a reporter of pH<sub>i</sub> for cardiac examinations. The following is a description of some of the unknowns in this field.

## 1.1 | pH<sub>i</sub> change: Cause or effect?

To the best of our knowledge, prior literature does not provide a comprehensive understanding of the relationship between intracellular pH and in-cell LDH and PDH activities in a living system. In states such as ischemia, there is a reduction of available oxygen and nutrients and reduced

washout of metabolites.<sup>4</sup> The reduction in pH in ischemia is attributed to several factors. First, the reduction in adenosine triphosphate (ATP), which is due to oxygen depletion and nutrient deprivation, reduces the activity of membrane-bound pH regulators of the cell, leading to a lower pH<sub>i</sub>.<sup>4</sup> Second, the reduction in washout of acidic metabolites that occurs in ischemia also reduces pH<sub>i</sub>.<sup>4</sup> Third, oxygen deprivation leads to a decrease in the NAD<sup>+</sup>/NADH ratio,<sup>30</sup> which in turn stimulates glycolysis and inhibits oxidative phosphorylation in the mitochondria. This metabolic shift is accompanied by increased LDH activity<sup>20–22</sup> and decreased PDH activity.<sup>21,22</sup> In one aspect, lactate, the product of pyruvate metabolism by LDH, is capable of lowering the tissue pH due to its low pK<sub>a</sub> of 3.78,<sup>31</sup> and lactate concentration was previously found to be correlated to both extracellular pH (pH<sub>e</sub>) and pH<sub>i</sub> in the rat brain during ischemia.<sup>32,33</sup> However, it is not known if increased lactate production under conditions that also involve acidification (such as stroke and ischemia<sup>20–22</sup>) is the cause of or is driven by intracellular acidification. In another aspect, PDH activity has been shown to decrease under ischemia that was accompanied by acidification in brain slices.<sup>21,22</sup> However, to the best of our knowledge, changes in PDH activity in muscle are not expected to be followed by changes in pH<sub>i</sub>.<sup>34</sup> To the best of our knowledge, it is yet unknown whether in-cell cardiac PDH activity is directly affected by pH<sub>i</sub>. Therefore, even though LDH, PDH, and pH<sub>i</sub> are changing simultaneously in ischemia, the direct effect of pH<sub>i</sub> reduction on LDH and PDH activities is not known.

# 1.2 | pH and high-energy phosphate nucleotides

LDH and PDH activities are both also affected by the ratios of high-energy phosphate nucleotides, such as nicotinamide adenine dinucleotides and adenosine triphosphates and diphosphates (NAD $^+$ /NADH and ATP/ADP). As pH<sub>i</sub> may affect these ratios, the interpretation and prediction of the response of LDH and PDH to changes in pH<sub>i</sub> is further complicated and may represent a balance between the direct effects of pH on these proteins and the indirect effects of pH<sub>i</sub>, which may lead to other intracellular changes that may affect these enzymes. To the best of our knowledge, these global effects of pH<sub>i</sub> on cardiac enzyme activities have not been studied before.

## 1.3 | Clinical relevance

In the clinical setting, acidosis of the blood and the extracellular space may occur in some patients as part of the etiology of several cardiac conditions and may induce a reduction in  $pH_i$  as well. In general, a reduction in cardiac pH leads to reduction in a heart contractility.<sup>3,5</sup> In agreement, global metabolic acidosis also affects the heart. Figure 1 summarizes the knowns and unknowns as regards  $pH_e$ ,  $pH_i$ , and their effects on in-cell metabolic enzyme activities.

The use of hyperpolarized  $[1^{-13}C]$  pyruvate is a promising modality for cardiac imaging and has shown utility in probing various conditions such as diabetic cardiomyopathy, <sup>12</sup> heart failure, <sup>36</sup> ischemia and ischemia/reperfusion injury, <sup>37</sup> and myocardial hypertrophy. <sup>11</sup> The current study may provide a better understanding of the processes that govern pyruvate metabolism in these conditions, with regard to the contribution of pH<sub>i</sub> reduction, which accompanies these conditions in some patients. This is key for correct interpretation of such cardiac studies using the production of  $[1^{-13}C]$  lactate and  $[^{13}C]$  bicarbonate as biomarkers.

## 1.4 | Methodological considerations

The methodology used to investigate the in-cell effect of  $pH_i$  on LDH and PDH activities in the isolated heart is briefly described in the following. The pharmacological challenges that were used to induce intracellular acidification are an  $NH_4CI$  prepulse (Figure S1) with or without a  $Na^+/H^+$  exchanger (NHE1) inhibitor. These were administered to the perfused mouse heart ex vivo. This investigatory system was chosen to isolate the effect of intracellular acidification on LDH and PDH activities. The perfused heart system (also known as the Langendorff heart<sup>38</sup>) enables acidification of the cardiac tissue, which may be less tolerated in vivo, and monitoring it without the effects of other organs' acidification. At the same time, this model system preserves an adequate physiologic cardiac function.

The mouse hearts were perfused inside an NMR spectrometer. This enabled pH determination using <sup>31</sup>P-NMR spectroscopy and LDH and PDH activity quantification using <sup>13</sup>C-NMR spectroscopy and hyperpolarized [1-<sup>13</sup>C]pyruvate. Oxygen consumption and temperature were monitored in tandem with the NMR spectroscopy recordings using NMR-compatible oxygen and temperature sensor systems.

# 2 | MATERIALS AND METHODS

Information on the materials and methods that were used in the current study and previously described<sup>29</sup>—including the chemicals; surgical procedure; perfusion system; NMR spectroscopy; hyperpolarized <sup>13</sup>C spectroscopy; DNP spin polarization and dissolution; tissue wet weight; LDH

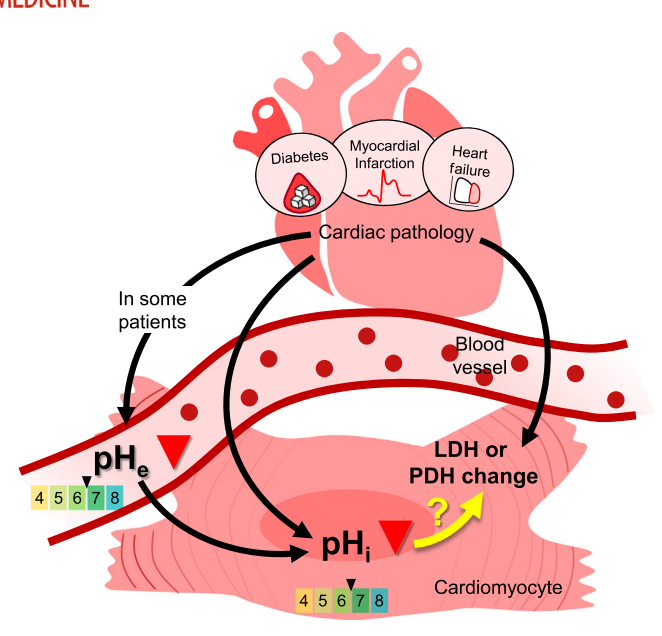


**FIGURE 1** Several cardiac conditions capable of damaging the heart consist of a reduction in pH<sub>i</sub> and, in some patients, also involve a reduction in pH<sub>e</sub>. These conditions are also known to be associated with changes in LDH and PDH activities. However, it is not known whether acidification of the intracellular space alone, without further insults, can lead to changes in LDH and PDH activities. LDH, lactate dehydrogenase; PDH, pyruvate dehydrogenase; pH<sub>e</sub>, extracellular pH; pH<sub>i</sub>, intracellular pH.

and PDH rate calculation;  $pH_i$  calculation; ATP and phosphocreatine (PCr) content quantification; and normalization of the enzymatic rates to ATP content—is provided in the supporting information (Note S1).

#### 2.1 | Animals

Male Institute for Cancer Research (ICR) mice (n = 30, 39–45 g) were obtained from the Institutional Authority of Biological and Biomedical Models. The joint ethics committee (Institutional Animal Care and Use Committee, IACUC) of the Hebrew University and Hadassah Medical Center approved the study protocol for animal welfare (protocol number MD-19-15827-1). The Hebrew University is an Association for Assessment and Accreditation of Laboratory Animal Care (AAALAC) international-accredited institute. Care was taken to minimize pain and discomfort to the animals. All procedures conformed to the guidelines from Directive 2010/63/EU of the European Parliament on the protection of animals used for scientific purposes.

# 2.2 Intracellular acidification with an NH<sub>4</sub>Cl prepulse and an NHE1 blocker

The NH<sub>4</sub>Cl prepulse is a well-established approach to induce intracellular acidification, which is achieved by adding NH<sub>4</sub>Cl and removing it after several minutes<sup>39</sup> (Figure S1). NHE1 accounts for approximately 60% of the proton removal capability of cardiac cells during intracellular acidification.<sup>40</sup> NHE1 on the plasma membrane co-transports H<sup>+</sup> out of the cytosol and Na<sup>+</sup> into the cytosol. Zoniporide was used here to reduce the pH<sub>i</sub> to a level that is lower than what would be achieved using the NH<sub>4</sub>Cl prepulse alone. The half maximal inhibitory concentration (IC<sub>50</sub>) of zoniporide is 14 nM,<sup>41</sup> and it was administered here at a concentration of 1  $\mu$ M; therefore, we may assume a complete inhibition of NHE1.

A detailed description on NH<sub>4</sub>Cl prepulse methodology and on NHE1 block is provided in Figure S1 and Note S1.

# 2.3 | Experimental workflow: Prior to the pharmacologic challenge

First, a  $^{31}$ P spectrum of oxygenated Krebs-Henseleit buffer (KH buffer) alone was acquired in the same NMR tube that was used for the rest of the experiment (10 mm diameter), at a flow rate that was used throughout the experiment. Then the mouse heart (n = 30) underwent aortic retrograde cannulation in vivo and was then isolated. The heart was then perfused with oxygenated KH buffer, at  $37^{\circ}$ C, using a peristaltic pump at a

constant flow rate of 7.5 mL/min. After confirming that the heart was beating spontaneously (visual), it was inserted into the NMR tube, then the tube with the beating heart fixed in it (as well as the sensors for temperature and  $O_2$  and the other perfusion lines) was lowered into the bore of the spectrometer.

## 2.4 | Experimental media

#### 2.4.1 | Solution 1

A modified version of KH buffer  $^{42}$  contains 10 mM glucose, 0.5 mM pyruvate, 118 mM NaCl, 4.7 mM KCl, 2 mM CaCl<sub>2</sub>, MgSO<sub>4</sub>, 25 mM NaHCO<sub>3</sub>, and 0.5 mM insulin in water (95/5 v/v double-distilled H<sub>2</sub>O/D<sub>2</sub>O). For Groups 4, 5, and 6, we used this KH buffer, which also contained 1.2 mM KH<sub>2</sub>PO<sub>4</sub>. For Groups 1, 2, and 3, we used a KH buffer that did not contain KH<sub>2</sub>PO<sub>4</sub>. This was done to allow clear visualization of the intracellular Pi signal without the overlapping signal of the extracellular Pi signal.

## 2.4.2 | Solution 2

Same as Solution 1, with the addition of 20 mM of  $NH_4CI$  (without osmotic compensation).<sup>43</sup> This solution was used to induce the  $NH_4CI$  prepulse.

## 2.4.3 | Solution 3

Same as Solution 1, with the addition of 20 mM of  $NH_4CI$  and 1  $\mu M$  of zoniporide. This solution was used to induce the  $NH_4CI$  prepulse with NHE1 inhibition.

# 2.4.4 | Solution 4

Same as Solution 1, with the addition of 1  $\mu$ M of zoniporide. This solution was used as a control to study the possible effects of zoniporide by itself on LDH and PDH activities.

All four solutions were freshly prepared for the various experimental conditions. During the experiments, the relevant solutions were kept in a water bath at  $40^{\circ}$ C outside the NMR spectrometer and were bubbled for 1 h prior to cardiac perfusion with 95%/5% O<sub>2</sub>/CO<sub>2</sub> at a flow rate of 3.5 L/min. The pH of these media was adjusted to be 7.4.

## 2.5 | Experimental groups according to pharmacologic challenges and data recording

 $NH_4Cl$  prepulse and zoniporide administration were used in conjunction or separately in six experimental groups, as described below and in Figure 2.

# 2.5.1 | Group 1: NH<sub>4</sub>Cl prepulse

This condition was induced by switching the perfusion from Solution 1 to Solution 2 for 24 min then switching back to Solution 1. <sup>31</sup>P spectroscopy was recorded to determine pH, ATP, and PCr. Dissolved oxygen (DO) was measured throughout.

# 2.5.2 | Group 2: NH<sub>4</sub>Cl prepulse with NHE1 inhibition

This condition was induced by switching the perfusion from Solution 1 to Solution 3 for 24 min, then switching to Solution 4 for 10 min, and then switching back to Solution 1. <sup>31</sup>P spectroscopy was recorded to determine pH, ATP, and PCr. DO was measured throughout.

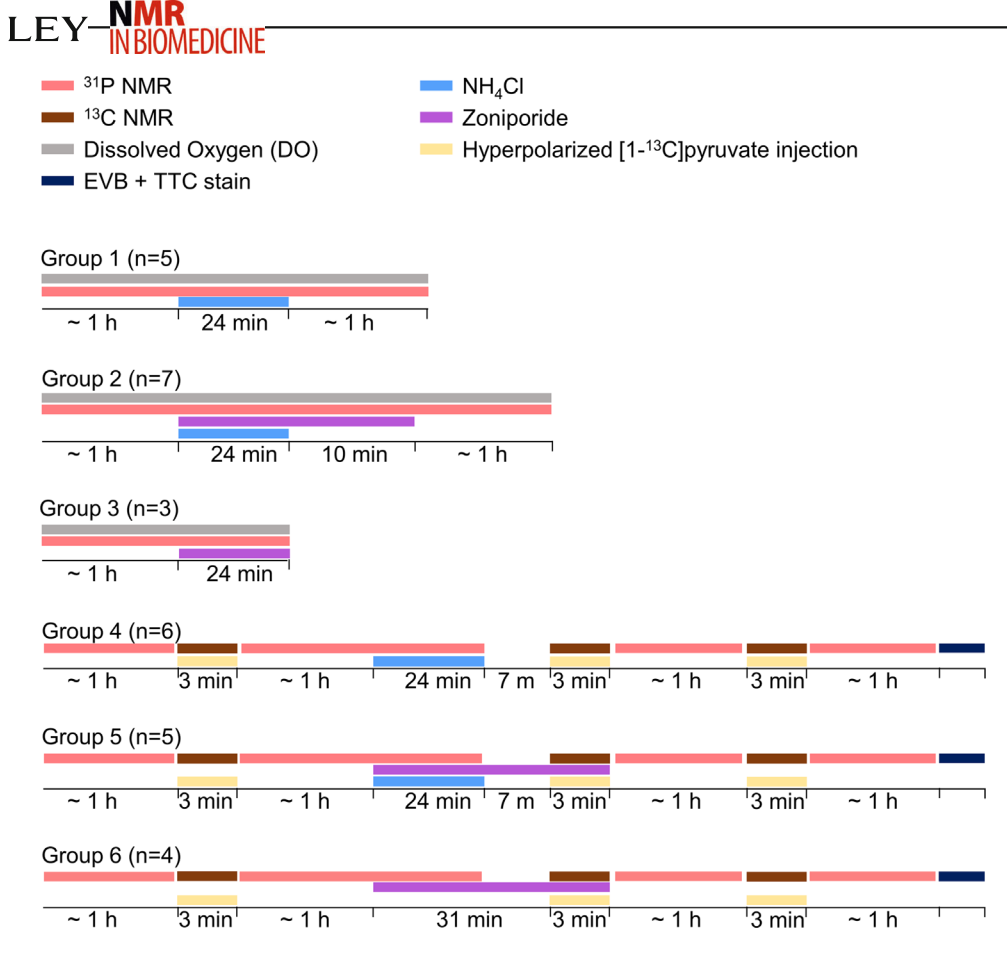


FIGURE 2 The experimental design. In Groups 1–3,  $^{31}P$  spectroscopy and dissolved oxygen measurement were performed in perfused mouse hearts. Baseline data were acquired for approximately 1 h, followed by three different pharmacological conditions, as indicated in the timeline: Group 1, NH<sub>4</sub>Cl prepulse (n = 5); Group 2, NH<sub>4</sub>Cl prepulse combined with zoniporide (n = 7); and Group 3, only zoniporide (n = 3). In Groups 1 and 2, recovery data were acquired as well for approximately 1 h. In Groups 4–6,  $^{31}P$  and  $^{13}C$  spectroscopy were performed in perfused mouse hearts (n = 15).  $^{31}P$  data were acquired for approximately 1 h and this was followed by  $^{13}C$  acquisition of the first hyperpolarized [1- $^{13}C$ ] pyruvate injection to obtain the baseline metabolic activity of LDH and PDH. Then three different conditions were applied before the second hyperpolarized [1- $^{13}C$ ] pyruvate injection, as indicated in the timeline: Group 4, NH<sub>4</sub>Cl prepulse (n = 5); Group 5, NH<sub>4</sub>Cl prepulse combined with zoniporide (n = 6); and Group 3, only zoniporide (n = 4). A third hyperpolarized [1- $^{13}C$ ] pyruvate injection was then applied to obtain LDH and PDH activity in the recovery phase.  $^{31}P$  spectra were acquired in between, as indicated in the timeline. EVB and TTC stains were obtained at the end of each experiment in Groups 4–6. n = the number of hearts (and animals) investigated in each group. The time durations are not drawn to scale. EVB, Evan's blue; LDH, lactate dehydrogenase; PDH, pyruvate dehydrogenase; TTC, triphenyltetrazolium chloride.

# 2.5.3 | Group 3: NHE1 inhibition without NH<sub>4</sub>Cl prepulse

This condition was induced by switching the perfusion from Solution 1 to Solution 4 for 34 min. <sup>31</sup>P spectroscopy was recorded to determine pH, ATP, and PCr. DO was measured throughout.

# 2.5.4 | Group 4: NH<sub>4</sub>Cl prepulse, with real-time in-cell enzymatic activity recording

This condition was induced as described for Group 1. In addition, LDH and PDH activities were recorded 1 h before the switch to Solution 2 and then 7 min and 1 h after the removal of Solution 2.

# 2.5.5 | Group 5: NH<sub>4</sub>Cl prepulse and NHE1 inhibition, with real-time in-cell enzymatic activity recording

This condition was induced as described for Group 2. In addition, LDH and PDH activities were recorded 1 h before the switch to Solution 3, and then 7 min after the switch to Solution 4, and 1 h after the switch back to Solution 1.

# 2.5.6 | Group 6: NHE1 inhibition without NH<sub>4</sub>Cl prepulse, with real-time in-cell enzymatic activity recording

This condition was induced as described for Group 3. In addition, LDH and PDH activities were recorded 1 h before the switch to Solution 4, and then 31 min after the switch to Solution 4, and 1 h after the switch back to Solution 1.

# 2.6 Demonstration of flow dynamics

To determine the flow characteristics of the hyperpolarized [ $1^{-13}$ C]pyruvate during the injection, we used the decrease in the water  $^{1}$ H signal during a D<sub>2</sub>O injection, as previously described. To this end, we injected a volume of 26 mL, composed of 20.8 mL of Solution 1 (80%) and 5.2 mL of D<sub>2</sub>O (20%), into the NMR tube, using the same continuous flow system as the hyperpolarized injections. The integrated intensity of the water  $^{1}$ H signal was inversed then normalized to demonstrate the flow characteristics that would correlate with the administration of the hyperpolarized substrate.

# 2.7 Data analysis and statistics

Spectral processing and statistical analysis are provided in Note \$1.

#### 2.8 | Measurement of DO

DO in the buffer was measured by O<sub>2</sub> sensor spots (Sticker type: Pst7-10), with an NMR-compatible fiber-optic DO meter (PreSens, Precision Sensing GmbH, Germany). Additional information is provided in Note S1.

# 2.9 Retrograde perfused heart staining and analysis

To ensure that the ATP content is a true surrogate for the amount of living cells in the heart, we performed a triphenyltetrazolium chloride (TTC) and an Evan's blue (EVB) staining of the isolated heart at the end of each experiment with Groups 4, 5, and 6. TTC staining is a well-established method to assess tissue viability, as such tissue turns red by mitochondrial dehydrogenases.<sup>44</sup> The EVB staining is an efficient tool with which to assess tissue perfusion.<sup>44</sup> The combination of both staining techniques was used to assess the proportion of tissue that is either perfused or not perfused but metabolically active, and thus informs regarding the percentage of the cardiac tissue that participated in [1-<sup>13</sup>C]pyruvate metabolism. Additional information on the staining procedures and the viability quantification is provided in Note S1.

## 3 | RESULTS

# 3.1 | LDH and PDH rate calculation

Using product-selective saturating-excitation pulses, <sup>45</sup> the hyperpolarized metabolites [1-<sup>13</sup>C]lactate and [<sup>13</sup>C]bicarbonate were fully sampled (and depolarized) by each selective pulse, and only newly synthetized metabolites were detected on each excitation. This enabled absolute quantification of the LDH and PDH activities on each injection. Figure 3 summarizes the acquisition and processing steps that enabled these enzymatic activity determinations. Further information is provided in Note S1.

# 3.2 Demonstration of flow dynamics

To study the flow characteristics of hyperpolarized  $[1^{-13}C]$  pyruvate during injection, we utilized the reduction in the water  $^1H$  signal during a  $D_2O$  injection (section 2.6). Figure  $^3C$  demonstrates one such  $D_2O$  injection and  $^4S$  (n=15, three injections each) individual effective relaxation time constant ( $T_{eff}$ ) corrected  $[1^{-13}C]$  pyruvate signal time courses. A high similarity is demonstrated in the wash-in and the plateau phases of both flow profiles. In the washout phase, it appears that the  $T_{eff}$  correction signal curve is variable, and with less agreement with the profile calculated based

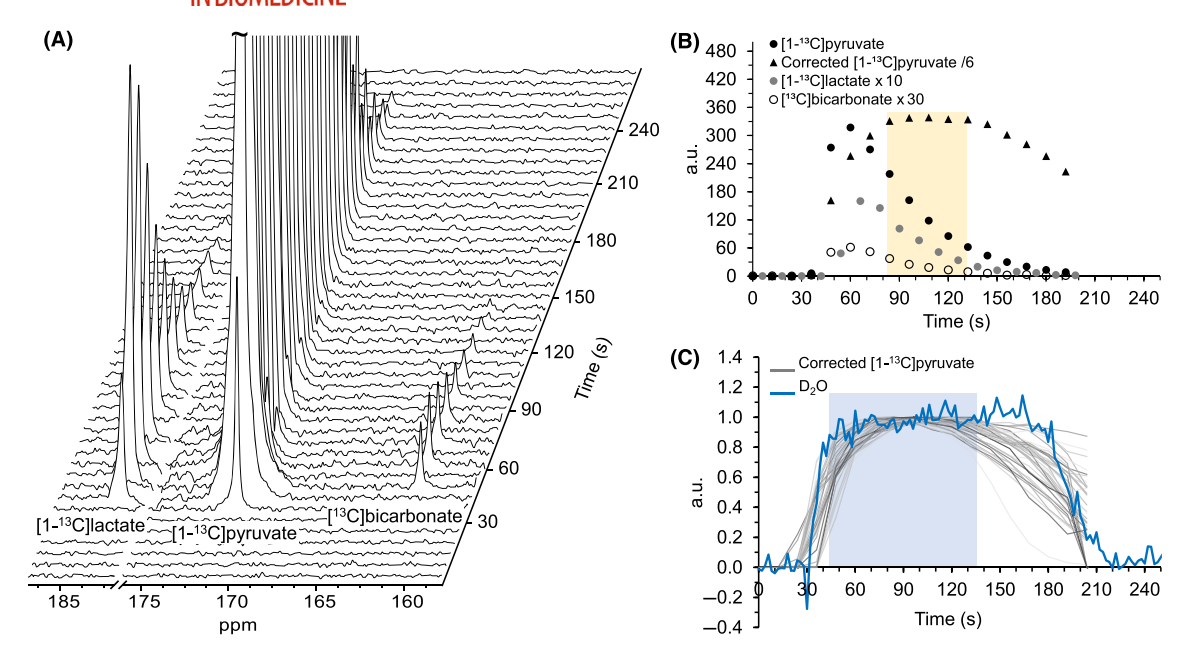


**FIGURE 3** Demonstration of processing and analysis of hyperpolarized  $[1^{-13}C]$  pyruvate metabolism. (A) Representative  $^{13}C$  NMR spectra of 14 mM hyperpolarized  $[1^{-13}C]$  pyruvate (171 ppm) injection to a heart and subsequent  $[1^{-13}C]$  lactate (183.2 ppm) and  $[^{13}C]$  bicarbonate (161.1 ppm) formation. The  $[1^{-13}C]$  pyruvate signal is truncated for better visualization of the smaller signals. The  $[1^{-13}C]$  pyruvate-hydrate signal (179.4 ppm) is not shown for clarity of the display. Time 0 is the time of dissolution of the hyperpolarized material. (B) Time courses of the denoised signal integrals of the signals in (A). Black circles,  $[1^{-13}C]$  pyruvate; black triangles,  $T_{\rm eff}$  corrected  $[1^{-13}C]$  pyruvate, reduced 6-fold for display; gray circles,  $[1^{-13}C]$  lactate, multiplied 10-fold for display; empty circles,  $[1^{3}C]$  bicarbonate, multiplied 30-fold for display. The temporal time window that contains the first four datapoints of constant  $[1^{-13}C]$  pyruvate concentration in this specific experiment, is highlighted. Only  $[1^{-13}C]$  lactate and  $[1^{3}C]$  bicarbonate datapoints from this time frame were used for the calculation of LDH and PDH activities. (C) Flow dynamics in the continuous perfusion system demonstrated using a  $D_2O$  injection. Each gray line corresponds to an individual,  $T_{\rm eff}$  corrected  $[1^{-13}C]$  pyruvate signal time course, normalized to its maximal value (altogether, 45 time courses, n=15 hearts, three hyperpolarized injections to each heart). The blue line corresponds to the inversed and normalized integral of the  $^{1}H$  signal during the  $D_2O$  injection. The highlighted time frame (48–132 s) is the time from dissolutions in which the  $T_{\rm eff}$  corrected  $[1^{-13}C]$  pyruvate signal were used for the calculation of LDH and PDH rates. LDH, lactate dehydrogenase; PDH, pyruvate dehydrogenase;  $T_{\rm eff}$ , effective relaxation time constant.

on the  $D_2O$  injection. This variability could reflect the cumulative effects of RF pulsation, variable  $T_1$  decay inside and outside the magnet, and possibly also substrate consumption. Nevertheless, this part of the experimental dataset was not used for enzymatic rates determinations.

# 3.3 | NH<sub>4</sub>Cl prepulse induces intracellular acidification

Figure 4 shows typical changes in  $^{31}P$  NMR spectra during an NH<sub>4</sub>Cl prepulse, which was performed in Group 1. As expected, the cardiac intracellular Pi (Pi<sub>(i)</sub>) signal shifted downfield (to the right) during the NH<sub>4</sub>Cl removal, indicating intracellular acidification.

In Group 1, the NH<sub>4</sub>Cl prepulse led to an intracellular acidification of  $0.18 \pm 0.09$  units at time T<sub>inj</sub> (indicated by yellow stripes in Figure 5A; p = 0.004 compared with baseline, two-tailed, paired, Student's t-test, n = 5). Combining the NH<sub>4</sub>Cl prepulse with NHE1 inhibition (zoniporide) in Group 2 led to a substantial drop in pH<sub>i</sub> of  $0.43 \pm 0.07$  units at the same time (T<sub>inj</sub>, p = 0.001, compared with baseline, two-tailed, paired, Student's t-test, n = 7; Figure 5D). These results are in line with previous studies that showed a more pronounced drop in pH<sub>i</sub> upon NH<sub>4</sub>Cl prepulse with NHE1 inhibition compared with the NH<sub>4</sub>Cl prepulse alone. At the same time, we could not detect any changes in ATP or PCr levels (Figure 5B,C,E,F). Addition of zoniporide alone (which did not induce intracellular acidification) did not lead to changes in the levels of either ATP or PCr (Figure S3).

The second hyperpolarized [ $1^{-13}$ C]pyruvate injection, which was aimed at investigating metabolism under the intracellular acidification condition, was performed during the time  $T_{inj}$ , which showed maximal intracellular acidification for both conditions (as indicated by the yellow stripes in Figures 4 and 5).

**FIGURE 4** Typical  $^{31}$ P NMR spectra of an isolated heart during an NH<sub>4</sub>Cl prepulse challenge (Group 1). Each spectrum was acquired within 7.5 min and shows the following metabolites: a, intracellular Pi<sub>(i)</sub>; b, PCr; c, γ-ATP + β-ADP; d, α-ATP + α-ADP; e, β-ATP. Spectra #1–3 were acquired before applying the NH<sub>4</sub>Cl prepulse (baseline). Spectra #4–6 were acquired during perfusion with a medium that contained 20 mM NH<sub>4</sub>Cl. Spectra #7–12 were acquired further to the removal of NH<sub>4</sub>Cl. The dashed line marks the center of the baseline cardiac Pi<sub>(i)</sub> signal to assist in visualizing the tissue acidification during the NH<sub>4</sub>Cl removal period. For each spectrum, the calculated pH value is provided on the left. The spectrum highlighted in yellow stripes was acquired at the time when the pH<sub>i</sub> was the lowest (maximal acidification). This time is marked T<sub>inj</sub> and is referred to in Figure 5. ADP, adenosine diphosphate; ATP, adenosine triphosphate; PCr, phosphocreatine; pH<sub>i</sub>, intracellular pH.

## 3.4 TTC and EVB staining correlate to the ATP content of the hearts

The combined staining method of TTC and EVB was used to discriminate between the metabolically active and nonactive regions of the heart (Note S1). Figure 6 shows the correlation between the metabolically active regions (area of perfused myocardium [AOP] + area at risk [AAR]) and the ATP content of the heart (determined during 52 min prior to the staining). This result suggested that the ATP content of the heart indeed provides an adequate surrogate to the amount of viable tissue in the heart.

## 3.5 | Pyruvate metabolism during intracellular acidification and NHE1 inhibition

The product-selective saturating-excitations acquisition approach was used for acquiring the hyperpolarized data and calculating LDH and PDH rates. In Groups 4–6, hyperpolarized [1-<sup>13</sup>C]pyruvate was injected three times into each perfused heart. The first injection was used as a baseline, the second injection was performed during the pharmacological challenge or control, and the third injection was used as a second control further to recovery from the pharmacological challenge.

The NH<sub>4</sub>Cl prepulse challenge (moderate intracellular acidification) led to a 16% reduction in LDH activity (p = 0.04, n = 6; Figure 7A) and to a 39% reduction in PDH activity (p = 0.001, n = 6; Figure 7B). In agreement, the LDH/PDH activities ratio increased by 41% (p = 0.02, n = 6; Figure 7C). The combined NH<sub>4</sub>Cl prepulse and zoniporide challenge (severe intracellular acidification) led to a 29% reduction in LDH activity (p = 0.01, p = 0.

We note that there was no change between injections 1 and 3 in any of the groups (Figure 7). This is reassuring in two aspects: (1) that the hearts have indeed recovered from the pharmacological challenges; and (2) that the standardization of the enzymatic activity results to the ATP content, which was measured throughout the experiment, was a useful tool to correct for the loss of viable regions in each heart over the experimental day. For comparison, the data are presented without this standardization to ATP content in Figure S4.

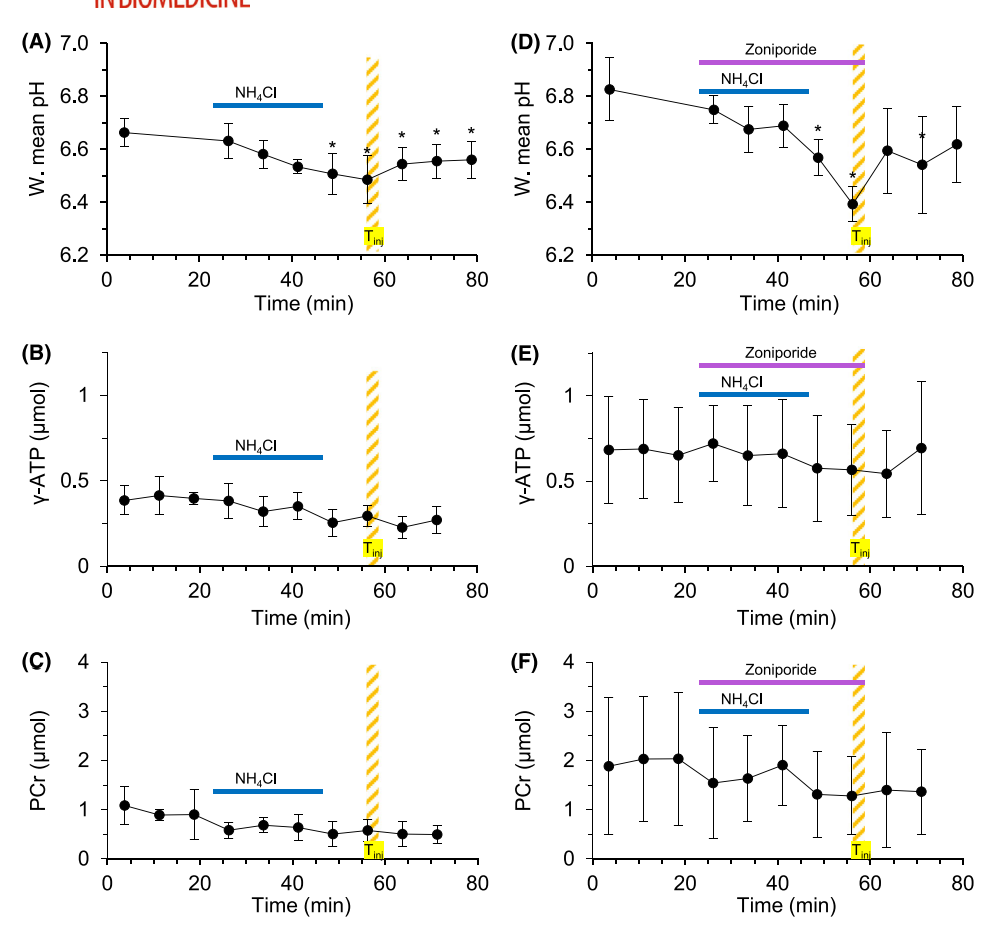


**FIGURE 5** Changes in pH<sub>i</sub>, ATP, and PCr during an NH<sub>4</sub>Cl prepulse with or without zoniporide. (A–C) Weighted mean pH<sub>i</sub>, ATP, and PCr, respectively, during the experiment with Group 1, which consisted of an NH<sub>4</sub>Cl prepulse. (D–F) Weighted mean pH<sub>i</sub>, ATP, and PCr, respectively, during the experiment with Group 2, which consisted of an NH<sub>4</sub>Cl prepulse combined with zoniporide. In (A,C,E), each datapoint is an average of n = 4 experimental days; in (B), each datapoint is an average of n = 5 experimental days; and in (D,F), each datapoint is an average of n = 7 experimental days. Each datapoint was acquired for 7.5 min using <sup>31</sup>P spectroscopy. Values are expressed as mean  $\pm$  standard deviation. The yellow stripes show the time duration  $T_{inj}$ , which indicates the time of second hyperpolarized [1-<sup>13</sup>C]pyruvate injection in Groups 4–6. Significance was tested compared with the baseline values (the first point on each plot), with a two-tailed, paired, Student's t-test (\* $p \le 0.05$ ; individual values for  $T_{inj}$  are provided in the text). ADP, adenosine diphosphate; ATP, adenosine triphosphate; PCr, phosphocreatine; pH<sub>i</sub>, intracellular pH.

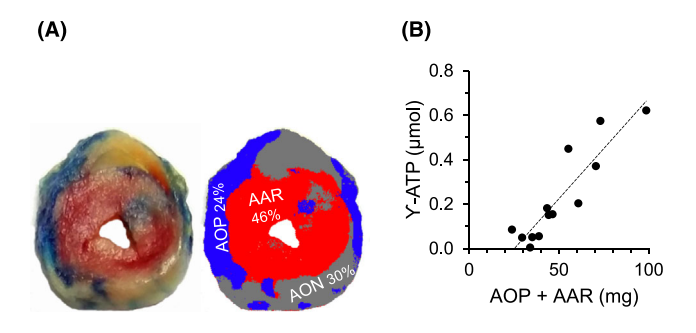
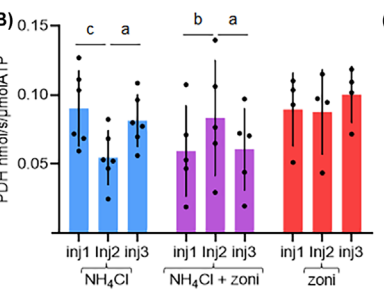
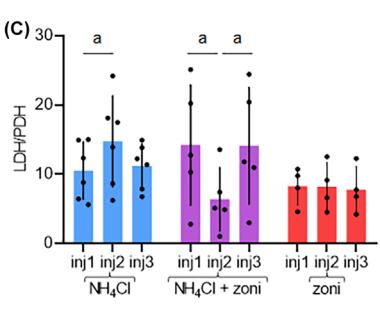


FIGURE 6 TTC and EVB staining of a typical isolated heart, and the correlation to γ-ATP. (A) Left: a typical axial slice of an isolated heart that was stained with TTC and EVB. Right: viability quantification performed by contouring the three-color subsets: blue, AOP; red, AAR; gray, AON; the white area is the ventricle lumen. The relative areas of the blue, red, and gray subsets were obtained using a pixel count tool and the weight of each region was calculated as described in the Methods. (B) Linear correlation ( $R^2 = 0.82$ ) between the AOP + AAR weight to the γ-ATP content of the heart. AAR, area at risk; AON, area of necrosis; AOP, area of perfusion; ATP, adenosine triphosphate; EVB, Evan's blue; TTC, triphenyltetrazolium chloride.





**FIGURE 7** The effect of NH<sub>4</sub>Cl prepulse and zoniporide on LDH, PDH, and LDH/PDH activities. Data were obtained from  $^{13}$ C spectroscopy of three hyperpolarized [1- $^{13}$ C] pyruvate injections (inj). The second injection of each heart was performed under three different conditions: Group 4, NH<sub>4</sub>Cl prepulse (blue, n = 6); Group 5, NH<sub>4</sub>Cl prepulse combined with zoniporide addition (purple, n = 5); and Group 6, zoniporide addition only (red, n = 4). The first and third injections to each heart were performed under regular buffer perfusion without NH<sub>4</sub>Cl or zoniporide. (A and B) LDH and PDH activities, respectively, normalized to the ATP content before each injection, expressed in nmol/s/ $\mu$ mol ATP. (C) LDH/PDH activities ratio. Values are shown as mean  $\pm$  standard deviation. Significance was tested by one-way ANOVA with repeated measures followed by Fisher's LSD post hoc test (a,  $p \le 0.05$ ; b, p < 0.01; c, p < 0.005; individual values are provided in the text). The LDH, PDH, and ATP values comprising the analysis shown here are provided in Table S1. ANOVA, analysis of variance; ATP, adenosine triphosphate; LDH, lactate dehydrogenase; LSD, least significant difference; PDH, pyruvate dehydrogenase; zoni, zoniporide.

# 3.6 DO concentration during NH<sub>4</sub>Cl prepulse with and without zoniporide

The DO that was associated with myocardial consumption ( $\Delta DO_{heart}$ ) was determined, as described in Note S1 and in Figure S5. Briefly,  $\Delta DO_{heart}$  was determined in three experimental groups (Figures 2 and S5): (1) in Group 1, before the NH<sub>4</sub>Cl prepulse (control, n = 3); (2) in Group 1, during the NH<sub>4</sub>Cl prepulse (n = 5); and (3) in Group 2, during NH<sub>4</sub>Cl prepulse with zoniporide (n = 7). We could not detect significant changes in the  $\Delta DO_{heart}$  in any of the conditions; however, we note that some of these measurements were noisy. The data are shown in Figure S5.

## 4 | DISCUSSION

## 4.1 | Clinical relevance

During states of myocardial dysfunction, the metabolic activity of the heart is changing, and consequently, LDH and PDH may be impacted. pH<sub>i</sub> may be impaired as a result of intracellular mechanisms,<sup>4</sup> and because of a systemic reaction to the cardiac dysfunction, which is followed by metabolic acidosis. In addition, metabolic acidosis may affect the heart by mechanisms that are unrelated to pH<sub>i</sub>. There are several clinical scenarios that entangle heart conditions and acidosis. For example, heart failure is usually accompanied by metabolic alkalosis due to drug use and neurohumoral mechanisms; however, metabolic acidosis can develop in end-stage heart failure because of reduced plasma renal flow and renal failure<sup>47</sup>; during acute myocardial infarction, the drop in cardiac output could cause metabolic acidosis as a result of tissue hypoxia<sup>48,49</sup>; genetic hypertension could cause hypertrophy and at the same time can be associated with metabolic acidosis<sup>50</sup>; and diabetes could lead to metabolic acidosis through diabetic nephropathy<sup>51</sup> and diabetic ketoacidosis.<sup>52</sup>

Metabolic acidosis was associated with an increased risk for ischemic heart disease and heart failure. Multiple factors may contribute to this association, although the exact mechanism is uncertain. The possible factors are decreased cardiac output, inflammation, activation of the reninangiotensin–aldosterone system, an increase in intracellular calcium that leads to proteolysis, hormones such as adrenaline, cortisol, and glucagon that cause supply–demand mismatch, and arrhythmias.  $^{53-56}$  Therefore, it is important to understand the in-cell effects of pH<sub>i</sub> reduction on cardiac metabolic enzyme activities.

# 4.2 New enzyme activity characteristics

In vitro studies in cell-free systems and purified enzymes report conflicting results as regards the dependence of LDH activity on pH. A study by Winer and Schwert showed that a pH drop within the range of approximately 10–5.5 increased LDH activity,<sup>57</sup> while a study by Javed et al.<sup>58</sup> reported that the LDH activity decreased with decreasing pH in the range of 7–4, and a study by Vesel et al. reported on two opposite trends for the LDH isozymes LDH1 and LDH5 in the pH range of 6.9–7.9.<sup>26</sup> For PDH, a pH drop in the range of approximately 8–7 was shown to reduce its activity.<sup>27</sup> Here, a drop of 0.2 units in pH<sub>i</sub> (from pH = 6.67) resulted in a modest decrease in LDH activity and a substantial decrease in PDH

activity. A larger drop in  $pH_i$  (from pH = 6.83) led to a more pronounced decrease in LDH activity and the PDH activity increased rather than decrease. Therefore, in both cases (the modest and the substantial pH decrease), the LDH activity decreased. However, PDH activity decreased on one challenge ( $NH_4CI$  prepulse), but increased on the other challenge ( $NH_4CI$  prepulse and zoniporide). These results could not be expected based on isolated enzyme studies. Therefore, first and foremost, this study demonstrates the importance of in-cell studies in real time. LDH and PDH act within a cellular microenvironment, and their real-time activities may be affected by multiple factors that act within that microenvironment and may be missing in cell-free systems.

Several factors may explain the results obtained in the current study. LDH is a cytosolic enzyme, and its activity is mainly influenced by the type of isozymes present and substrate availability. In the current (forward) reaction, the relevant substrates are pyruvate and NADH. As pyruvate is given in excess, the decrease in LDH activity may be explained by (1) the presence of LDH isozymes that decrease in activity upon pH reduction; and (2) a decrease in NADH or its binding affinity or by an excess of NAD<sup>+</sup>.

As regards PDH activity, reduced contractile function was previously observed during intracellular and extracellular acidification and was attributed to the increase in sarcolemma-free  $Ca^{+2}$  ions. <sup>59-61</sup> Reduced contractile function may reduce the ATP usage and the ATP/ADP ratio may increase. The latter may activate pyruvate dehydrogenase kinase, which in turn will deactivate PDH. <sup>62</sup> This process may, in addition to the response of the isolated PDH enzyme to pH reduction, explain the decrease in PDH activity observed further to the NH<sub>4</sub>Cl prepulse.

However, these mechanisms cannot explain the increased PDH activity observed under the lower pH<sub>i</sub>, which was induced by the combination of the NH<sub>4</sub>Cl prepulse and zoniporide. We propose the following explanation for this observation. In the inner mitochondrial membrane, NHE1 transports H<sup>+</sup> into the mitochondrion and co-transport Na<sup>+</sup> to the cytosol. This is opposed to its activity in the plasma membrane, which transports H<sup>+</sup> out of the cytosol into the extracellular space and transports Na<sup>+</sup> into the cytosol<sup>63</sup> (Figure S2). Because of NHE1 inhibition by zoniporide, H<sup>+</sup> is likely to accumulate in the cytosol, but not in the mitochondrion. Therefore, the use of the NH<sub>4</sub>Cl prepulse acidification approach combined with NHE1 inhibition likely leads to an increased proton gradient across the mitochondrial membrane. This gradient may enhance the activity of other co-transporters that rely on this proton gradient. One such co-transporter is the mitochondrial pyruvate carrier.<sup>64-67</sup> In this case, pyruvate concentration will increase in the mitochondrion and decrease in the cytosol. The increased mitochondrial pyruvate concentration will provide more substrate to the PDH reaction and therefore will lead to increased PDH activity (manifesting as increased production of hyperpolarized [<sup>13</sup>C] bicarbonate), in agreement with the current results. This increased transport of pyruvate into the mitochondria may lead to reduced availability of pyruvate in the cytosol (compared with the same state without NHE1 inhibition). This may lead to reduced LDH activity (manifesting as reduced hyperpolarized [1-<sup>13</sup>C]lactate production), in agreement with the current results. This proposed mechanism is illustrated in Figure S6.

Previously, we have reported on a correlation between the cardiac tissue pH and the LDH/PDH activities ratio in the pH range of approximately 6.6–7.2, where a decrease in pH led to an increase in this ratio.<sup>29</sup> Such a trend was also demonstrated previously in an ischemia/reperfusion injury model.<sup>37</sup> The advantages of using the LDH to PDH ratio are mainly attributable to its independence of quantification factors, such as the amount of viable tissue.<sup>29</sup> However, we now show that the use of this ratio may mask the events that underlie it and even lead to opposite conclusions. Here, we have shown that upon mild acidification, the LDH/PDH ratio indeed increased. However, both enzymatic activities decreased, with PDH decreasing more than the decrease in LDH. In the case of severe acidification, the LDH/PDH ratio showed an opposite trend to the previously observed correlation.<sup>29</sup>

## 4.3 | Significance of this study

The findings of this study could be used in the future to discriminate states of intracellular acidification from other cardiac conditions. For example, it might be implemented to differentiate between heart regions that suffered an ischemic injury, characterized by increased LDH and reduced PDH,<sup>37</sup> from the rest of the heart, which might be exposed to a systemic metabolic acidosis as a result of systemic tissue hypoxia that is secondary to the reduced cardiac output.<sup>48,49</sup>

There are indications that NHE1 inhibition might be beneficial in the treatment of cardiac injury caused by sepsis, hypovolemic circulatory shock, and certain forms of metabolic acidosis.<sup>68–70</sup> In this study, we have shown that NHE1 inhibition during intracellular acidosis is characterized by increased PDH activity, which likely increases aerobic respiration. This may provide an explanation for the beneficial effects of NHE1 inhibition.

## 4.4 | Limitations

# 4.4.1 | $\Delta DO_{heart}$ determination

In this study, we could not detect changes in  $\Delta DO_{heart}$  during the NH<sub>4</sub>Cl prepulse with or without zoniporide, although oxygen consumption is expected to decrease following the reduction of pH<sub>e</sub> to 6.8.<sup>71</sup> However, our inability to detect changes in  $\Delta DO_{heart}$  could be related to the noisy data that were obtained.



# 4.4.2 | Nonworking heart

The current study was performed in a Langendorff heart preparation, which does not work against resistance. Olson et al.<sup>72</sup> have conducted a study that investigated metabolic changes in a working (i.e., against resistance) versus Langendorff mouse heart. In the working heart preparation, the inflow goes through the left atrium, and the outflow goes through the aorta; left ventricular pressure is measured through the apex; and the preload and afterload are controlled. The Langendorff preparation used by Olson et al.<sup>72</sup> was similar to the Langendorff preparation used in our study, except for measurement of left ventricular pressure through the apex. The working heart showed higher oxygen consumption, which likely indicates increased PDH activity, along with increased glycolysis.<sup>72</sup> Nevertheless, it is unclear whether the balance between LDH and PDH activity is different in the working heart compared with the Langendorff heart. In addition, it is interesting to note that Park et al.<sup>73</sup> have demonstrated increased PDH activity in a working skeletal muscle compared with a resting muscle. Based on these two studies, we believe that is reasonable to assume that the base PDH and LDH activities are higher in the working heart compared with the Langendorff heart; however, the relative activities are not likely to be different. In this context, we believe that the results obtained here in the Langendorff heart, as regards changes in the relative activities of LDH and PDH upon intracellular acidification of various degrees, will hold in the working heart as well.

# 4.4.3 | Determination of regional perfusion and the effects on pH<sub>i</sub> determination

The determinations of AOP, AAR, and AON were performed at the end of each experimental day, after several hours of heart perfusion in the NMR spectrometer. A typical example is shown in Figure 6 and demonstrates relatively low AOP (24%) and AAR (46%). However, because these measurements were made at the end of the day, they do not reflect the perfusion status and tissue viability throughout the entire duration of the experiment. The perfusion and viability typically degrade over time, as evidenced by the ATP content. This is because vessel occlusion may occur over time. In the experiments that were used to measure the pH changes (Groups 1–3), there was no Pi in the medium during the acidification protocol. Therefore, the pH measured by the <sup>31</sup>P signal of Pi, primarily reflected the intracellular environment. In addition, it is important to note that regions of the heart that were not perfused were also not expected to exhibit pH<sub>i</sub> changes after NH<sub>4</sub>Cl prepulse, as the NH<sub>4</sub>Cl was not delivered to these regions. Therefore, it is important to consider the change in pH<sub>i</sub> rather than the absolute pH<sub>i</sub> values in this study when interpreting the results.

## 5 | CONCLUSIONS

In-cell pyruvate metabolism was monitored under intracellular acidosis with and without NHE1 inhibition. Our findings highlight the effect of intracellular acidification on LDH and PDH activities, which should be considered when interpreting hyperpolarized MRI cardiac results. We believe that understanding the relationship between intracellular acidification and LDH and PDH activities will enable better use of these enzymes as biomarkers and may also improve the diagnosis of additional cardiac conditions. This work may also pave the way for further understanding and improvement in NHE1 inhibitor treatment.

## **ACKNOWLEDGMENTS**

The authors wish to thank Dr. Ayelet Gamliel for experimental assistance. This project received funding from the Israel Science Foundation under grant agreement No. 1379/18, the Jabotinsky Scholarship of the Israeli Ministry of Science and Technology for Applied and Engineering Sciences for Direct PhD Students No. 3-15892 for D.S., and the European Union's Horizon 2020 research and innovation program under grant agreement No. 858149 (AlternativesToGd).

#### CONFLICT OF INTEREST STATEMENT

The authors have no conflict of interest.

## ORCID

Gal Sapir https://orcid.org/0000-0001-6267-5933

Rachel Katz-Brull https://orcid.org/0000-0003-4850-1616

## REFERENCES

- 1. Dixon M. The effect of pH on the affinities of enzymes for substrates and inhibitors. Biochem J. 1953;55(1):161-170. doi:10.1042/bj0550161
- Stigter D, Alonso DO, Dill KA. Protein stability: electrostatics and compact denatured states. Proc Natl Acad Sci U S A. 1991;88(10):4176-4180. doi:10.1073/pnas.88.10.4176

- 3. Williamson JR, Safer B, Rich T, Schaffer S, Kobayashi K. Effects of acidosis on myocardial-contractility and metabolism. *Acta Med Scand.* 1976; 199(S587):95-112. doi:10.1111/j.0954-6820.1976.tb05871.x
- Vaughan-Jones RD, Spitzer KW, Swietach P. Intracellular pH regulation in heart. J Mol Cell Cardiol. 2009;46(3):318-331. doi:10.1016/j.yjmcc.2008.
   10.024
- 5. Poole-Wilson PA. Regulation of intracellular ph in the myocardium relevance to pathology. *Mol Cell Biochem*. 1989;89(2):151-155. doi:10.1007/
- 6. Lewis AJM, Miller JJ, Lau AZ, et al. Noninvasive immunometabolic cardiac inflammation imaging using hyperpolarized magnetic resonance. *Circ Res.* 2018;122(8):1084-1093. doi:10.1161/CIRCRESAHA.117.312535
- Lauritzen MH, Magnusson P, Laustsen C, et al. Imaging regional metabolic changes in the ischemic rat heart in vivo using hyperpolarized [1-<sup>13</sup>C]pyruvate. Tomography. 2017;3(3):123-130. doi:10.18383/j.tom.2017.00008
- 8. Schroeder MA, Lau AZ, Chen AP, et al. Hyperpolarized <sup>13</sup>C magnetic resonance reveals early- and late-onset changes to in vivo pyruvate metabolism in the failing heart. *Eur J Heart Fail*. 2013;15(2):130-140. doi:10.1093/eurjhf/hfs192
- Yoshihara HA, Bastiaansen JA, Berthonneche C, Comment A, Schwitter J. An intact small animal model of myocardial ischemia-reperfusion: characterization of metabolic changes by hyperpolarized <sup>13</sup>C MR spectroscopy. Am J Physiol-Heart Circul Physiol. 2015;309(12):H2058-H2066. doi:10.1152/aipheart.00376.2015
- 10. Yoshihara HA, Bastiaansen JA, Berthonneche C, Comment A, Schwitter J. Assessing ischemic myocardial metabolism in vivo with hyperpolarized <sup>13</sup>C: relating the metabolic perturbation to the area at risk. *J Cardiovasc Magn Reson*. 2015;17(Suppl 1):O97. doi:10.1186/1532-429X-17-S1-O97
- 11. Seymour AM, Giles L, Ball V, et al. In vivo assessment of cardiac metabolism and function in the abdominal aortic banding model of compensated cardiac hypertrophy. Cardiovasc Res. 2015;106(2):249-260. doi:10.1093/cvr/cvv101
- 12. Le Page LM, Rider OJ, Lewis AJ, et al. Increasing pyruvate dehydrogenase flux as a treatment for diabetic cardiomyopathy: a combined C-13 hyperpolarized magnetic resonance and echocardiography study. *Diabetes*. 2015;64(8):2735-2743. doi:10.2337/db14-1560
- 13. Cunningham CH, Lau JYC, Chen AP, et al. Hyperpolarized C-13 metabolic MRI of the human heart initial experience. *Circ Res.* 2016;119(11):1177-1182. doi:10.1161/CIRCRESAHA.116.309769
- 14. Rider OJ, Apps A, Miller J, et al. Noninvasive in vivo assessment of cardiac metabolism in the healthy and diabetic human heart using hyperpolarized C-13 MRI. Circ Res. 2020;126(6):725-736. doi:10.1161/CIRCRESAHA.119.316260
- Ball DR, Cruickshank R, Carr CA, et al. Metabolic imaging of acute and chronic infarction in the perfused rat heart using hyperpolarised [1-<sup>13</sup>C]pyruvate. NMR Biomed. 2013;26(11):1441-1450. doi:10.1002/nbm.2972
- 16. Merritt ME, Harrison C, Sherry AD, Malloy CR, Burgess SC. Flux through hepatic pyruvate carboxylase and phosphoenolpyruvate carboxykinase detected by hyperpolarized 13C magnetic resonance. *Proc Natl Acad Sci U S A.* 2011;108(47):19084-19089. doi:10.1073/pnas.1111247108
- 17. Adler-Levy Y, Nardi-Schreiber A, Harris T, et al. In-cell determination of lactate dehydrogenase activity in a luminal breast cancer model ex vivo investigation of excised xenograft tumor slices using dDNP hyperpolarized 1-C-13 pyruvate. Sensors. 2019;19(9):2089. doi:10.3390/s19092089
- 18. Lev-Cohain N, Sapir G, Harris T, et al. Real-time ALT and LDH activities determined in viable precision-cut mouse liver slices using hyperpolarized 1-C-13 pyruvate-Implications for studies on biopsied liver tissues. *NMR Biomed*. 2019;32(2):e4043. doi:10.1002/nbm.4043
- 19. Lev-Cohain N, Sapir G, Uppala S, et al. Differentiation of heterogeneous mouse liver from HCC by hyperpolarized <sup>13</sup>C magnetic resonance. *Sci.* 2021; 3(1):8. doi:10.3390/sci3010008
- 20. Grieb B, Uppala S, Sapir G, Shaul D, Gomori JM, Katz-Brull R. Curbing action potential generation or ATP-synthase leads to a decrease in in-cell pyruvate dehydrogenase activity in rat cerebrum slices. *Sci Rep.* 2021;11(1):10211. doi:10.1038/s41598-021-89534-4
- 21. Sapir G, Shaul D, Lev-Cohain N, Sosna J, Gomori JM, Katz-Brull R. LDH and PDH activities in the ischemic brain and the effect of reperfusion—an ex vivo MR study in rat brain slices using hyperpolarized [1-13C]pyruvate. *Metabolites*. 2021;11(4):210. doi:10.3390/metabo11040210
- 22. Shaul D, Grieb B, Sapir G, et al. The metabolic representation of ischemia in rat brain slices: a hyperpolarized <sup>13</sup>C magnetic resonance study. *NMR Biomed*. 2021;34(7):e4509. doi:10.1002/nbm.4509
- 23. Sapir G, Steinberg DJ, Aqeilan RI, Katz-Brull R. Real-time non-invasive and direct determination of lactate dehydrogenase activity in cerebral organoids a new method to characterize the metabolism of brain organoids? *Pharmaceuticals*. 2021;14(9):878. doi:10.3390/ph14090878
- 24. Ardenkjaer-Larsen JH, Fridlund B, Gram A, et al. Increase in signal-to-noise ratio of > 10,000 times in liquid-state NMR. *Proc Natl Acad Sci U S A*. 2003;100(18):10158-10163. doi:10.1073/pnas.1733835100
- 25. Le Page LM, Rider OJ, Lewis AJ, et al. Assessing the effect of hypoxia on cardiac metabolism using hyperpolarized C-13 magnetic resonance spectroscopy. NMR Biomed. 2019;32(7):e4099. doi:10.1002/nbm.4099
- 26. Vesell ES, Fritz PJ, White EL. Effects of buffer, pH, ionic strength and temperature on lactate dehydrogenase isozymes. *Biochim Biophys Acta*. 1968; 159(2):236-243. doi:10.1016/0005-2744(68)90072-7
- 27. Pawelczyk T, Easom RA, Olson MS. Effect of ionic strength and pH on the activity of pyruvate dehydrogenase complex from pig kidney cortex. *Arch Biochem Biophys.* 1992;294(1):44-49. doi:10.1016/0003-9861(92)90134-I
- 28. Schulz E, Munzel T. Intracellular pH a fundamental modulator of vascular function. Circulation. 2011;124(17):1806-1807. doi:10.1161/CIRCULATIONAHA.111.061226
- 29. Shaul D, Azar A, Sapir G, et al. Correlation between lactate dehydrogenase/pyruvate dehydrogenase activities ratio and tissue pH in the perfused mouse heart: a potential noninvasive indicator of cardiac pH provided by hyperpolarized magnetic resonance. NMR Biomed. 2021;34(2):e4444. doi:10.1002/nbm.4444
- 30. Wengrowski AM, Kuzmiak-Glancy S, Jaimes R, Kay MW. NADH changes during hypoxia, ischemia, and increased work differ between isolated heart preparations. *Am J Physiol-Heart Circul Physiol*. 2014;306(4):H529-H537. doi:10.1152/ajpheart.00696.2013
- 31. HMDB. L-Lactic acid. 2022. Accessed January 30, 2022. http://www.hmdb.ca/metabolites/HMDB0000190
- 32. Gadian DG, Frackowiak RSJ, Crockard HA, et al. Acute cerebral-ischemia concurrent changes in cerebral blood-flow, energy metabolites, pH, and lactate measured with hydrogen clearance and P-31 and H-1 nuclear-magnetic-resonance spectroscopy. *J Cereb Blood Flow Metab.* 1987;7(2):199-206. doi:10.1038/jcbfm.1987.45
- 33. Katsura K, Asplund B, Ekholm A, Siesjo BK. Extracellular and intracellular pH in the brain during ischemia, related to tissue lactate content in normocapnic and hypercapnic rats. Eur J Neurosci. 1992;4(2):166-176. doi:10.1111/j.1460-9568.1992.tb00863.x

- 34. Kasper JD, Meyer RA, Beard DA, Wiseman RW. Effects of altered pyruvate dehydrogenase activity on contracting skeletal muscle bioenergetics. Am J Physiol Regul Integr Comp Physiol. 2019;316(1):R76-R86. doi:10.1152/ajpregu.00321.2018
- 35. Kane DA. Lactate oxidation at the mitochondria: a lactate-malate-aspartate shuttle at work. Front Neurosci. 2014;8:8. doi:10.3389/fnins.2014.00366
- 36. Bogh N, Hansen ESS, Omann C, et al. Increasing carbohydrate oxidation improves contractile reserves and prevents hypertrophy in porcine right heart failure. *Sci Rep.* 2020;10(1):8158. doi:10.1038/s41598-020-65098-7
- 37. Moon C-M, Kim Y-H, Ahn Y-K, Jeong M-H, Jeong G-W. Metabolic alterations in acute myocardial ischemia-reperfusion injury and necrosis using in vivo hyperpolarized [1-<sup>13</sup>C] pyruvate MR spectroscopy. *Sci Rep.* 2019;9(1):18427. doi:10.1038/s41598-019-54965-7
- 38. Lateef R, Al-Masri A, Alyahya A. Langendorff's isolated perfused rat heart technique: a review. Int J Basic Clin Pharmacol. 2015;4:1314-1322. doi:10. 18203/2319-2003.ijbcp20151381
- 39. Boron WF, Deweer P. Intracellular pH transients in squid giant-axons caused by CO2, NH3, and metabolic-inhibitors. *J Gen Physiol.* 1976;67(1):91-112. doi:10.1085/jgp.67.1.91
- Vaughan-Jones RD, Villafuerte FC, Swietach P, Yamamoto T, Rossini A, Spitzer KW. pH-Regulated Na(+) influx into the mammalian ventricular myocyte: the relative role of Na(+)-H(+) exchange and Na(+)-HCO Co-transport. J Cardiovasc Electrophysiol. 2006;17(Suppl 1):S134-s140. doi:10. 1111/j.1540-8167.2006.00394.x
- 41. Tracey WR, Allen MC, Frazier DE, et al. Zoniporide: a potent and selective inhibitor of the human sodium-hydrogen exchanger isoform 1 (NHE-1). *Cardiovasc Drug Rev.* 2003;21(1):17-32. doi:10.1111/j.1527-3466.2003.tb00103.x
- 42. Kolwicz SC, Tian R. Assessment of cardiac function and energetics in isolated mouse hearts using <sup>31</sup>P NMR spectroscopy. *J Vis Exp.* 2010;42(42): 2069. doi:10.3791/2069
- 43. Kaila K, Vaughanjones RD. Influence of sodium-hydrogen exchange on intracellular pH, sodium and tension in sheep cardiac purkinje-fibers. *J Physiol-London*. 1987;390(1):93-118. doi:10.1113/jphysiol.1987.sp016688
- 44. Redfors B, Shao Y, Omerovic E. Myocardial infarct size and area at risk assessment in mice. Experiment Clin Cardiol. 2012;17(4):268-272.
- 45. Harris T, Uppala S, Lev-Cohain N, et al. Hyperpolarized product selective saturating-excitations for determination of changes in metabolic reaction rates in real-time. NMR Biomed. 2020;33(2):e4189. doi:10.1002/nbm.4189
- 46. Hartmann M, Decking UK. Blocking Na<sup>+</sup>-H<sup>+</sup> exchange by cariporide reduces Na<sup>+</sup>-overload in ischemia and is cardioprotective. *J Mol Cell Cardiol*. 1999;31(11):1985-1995. doi:10.1006/jmcc.1999.1029
- 47. Urso C, Brucculeri S, Caimi G. Acid-base and electrolyte abnormalities in heart failure: pathophysiology and implications. *Heart Fail Rev.* 2015;20(4): 493-503. doi:10.1007/s10741-015-9482-y
- 48. Kirby BJ, McNicol MW. Acid-base status in acute myocardial infarction. Lancet. 1966;2(7472):1054-1056.
- 49. Wu MY, Yiang GT, Liao WT, et al. Current mechanistic concepts in ischemia and reperfusion injury. *Cell Physiol Biochem*. 2018;46(4):1650-1667. doi: 10.1159/000489241
- 50. Sharma AM, Distler A. Acid-base abnormalities in hypertension. Am J Med Sci. 1994;307:S112-S115.
- 51. Khairallah P, Scialla JJ. Role of acid-base homeostasis in diabetic kidney disease. Curr Diab Rep. 2017;17(4):28. doi:10.1007/s11892-017-0855-6
- 52. Dhatariya KK, Glaser NS, Codner E, Umpierrez GE. Diabetic ketoacidosis. Nat Rev Dis Primers. 2020;6(1):1. doi:10.1038/s41572-020-0165-1
- 53. Gandhi M, Suvarna TT. Cardiovascular complications in diabetic ketoacidosis. Int J Diab Dev Countries. 1995;15:132-133.
- 54. Kaefer K, Botta I, Mugisha A, et al. Acute coronary syndrome and diabetic keto acidosis: the chicken or the egg? *Ann Transl Med.* 2019;7(16):397. doi: 10.21037/atm.2019.07.38
- 55. Collister D, Ferguson TW, Funk SE, Reaven NL, Mathur V, Tangri N. Metabolic acidosis and cardiovascular disease in CKD. *Kidney Med.* 2021;3(5): 753-761.e1. doi:10.1016/j.xkme.2021.04.011
- Kraut JA, Nagami GT. Metabolic acidosis and cardiovascular disease. In: Wesson DE, ed. Metabolic Acidosis: A Guide to Clinical Assessment and Management. Springer New York; 2016:87-99.
- 57. Winer AD, Schwert GW. Lactic dehydrogenase: IV. The influence of pH on the kinetics of the reaction. *J Biol Chem.* 1958;231(2):1065-1083. doi:10.1016/S0021-9258(18)70467-5
- 58. Javed MH, Azimuddin SMI, Hussain AN, Ahmed A, Ishaq M. Purification and characterization of lactate dehydrogenase from Varanus liver. *Exp Mol Med.* 1997;29(1):25-30. doi:10.1038/emm.1997.4
- 59. Kanaya N, Murray PA, Damron DS. Propofol increases myofilament Ca2+ sensitivity and intracellular pH via activation of Na+-H+ exchange in rat ventricular myocytes. *Anesthesiology*. 2001;94(6):1096-1104. doi:10.1097/00000542-200106000-00026
- 60. Fabiato A, Fabiato F. Effects of pH on the myofilaments and the sarcoplasmic reticulum of skinned cells from cardiace and skeletal muscles. *J Physiol.* 1978;276(1):233-255. doi:10.1113/jphysiol.1978.sp012231
- 61. Schaffer SW, Safer B, Ford C, Illingworth J, Williamson JR. Respiratory acidosis and its reversibility in perfused rat heart: regulation of citric acid cycle activity. Am J Physiol. 1978;234(1):H40-H51. doi:10.1152/ajpheart.1978.234.1.H40
- 62. Pawelczyk T, Olson MS. Regulation of pyruvate-dehydrogenase kinase-activity from pig-kidney cortex. *Biochem J.* 1992;288(2):369-373. doi:10.1042/bj2880369
- 63. Ruiz-Meana M, Garcia-Dorado D, Pina P, Inserte J, Agullo L, Soler-Soler J. Cariporide preserves mitochondrial proton gradient and delays ATP depletion in cardiomyocytes during ischemic conditions. Am J Physiol-Heart Circulat Physiol. 2003;285(3):H999-H1006. doi:10.1152/ajpheart.00035.2003
- 64. Papa S, Francavilla A, Paradies G, Meduri B. The transport of pyruvate in rat liver mitochondria. FEBS Lett. 1971;12(5):285-288. doi:10.1016/0014-5793(71)80200-4
- 65. Halestrap AP. Pyruvate and ketone-body transport across the mitochondrial membrane. Exchange properties, pH-dependence and mechanism of the carrier. *Biochem J.* 1978;172(3):377-387. doi:10.1042/bj1720377
- 66. Halestrap AP. Stimulation of pyruvate transport in metabolizing mitochondria through changes in the transmembrane pH gradient induced by glucagon treatment of rats. *Biochem J.* 1978;172(3):389-398. doi:10.1042/bj1720389
- 67. de Andrade PBM, Casimir M, Maechler P. Mitochondrial activation and the pyruvate paradox in a human cell line. FEBS Lett. 2004;578(3):224-228. doi:10.1016/j.febslet.2004.10.088
- 68. Wu D, Arias J, Bassuk J, et al. Na+/H+ exchange inhibition delays the onset of hypovolemic circulatory shock in pigs. *Shock*. 2008;29(4):519-525. doi: 10.1097/SHK.0b013e318150757a
- 69. Wu D, Kraut JA. Role of NHE1 in the cellular dysfunction of acute metabolic acidosis. Am J Nephrol. 2014;40(1):36-42. doi:10.1159/000364783

10991492, 2023,

. 10, Downloaded

from https://analyticalscie

- 70. Kraut JA, Madias NE. Lactic acidosis: current treatments and future directions. Am J Kidney Dis. 2016;68(3):473-482. doi:10.1053/j.ajkd.2016.04.020
- 71. Pearce FJ, Walajtysrode E, Williamson JR. Effects of work and acidosis on pyruvate-dehydrogenase activity in perfused rat hearts. *J Mol Cell Cardiol*. 1980;12(5):499-510. doi:10.1016/0022-2828(80)90006-1
- 72. Olson AK, Bouchard B, Zhu WZ, Chatham JC, Des Rosiers C. First characterization of glucose flux through the hexosamine biosynthesis pathway (HBP) in ex vivo mouse heart. *J Biol Chem.* 2020;295(7):2018-2033. doi:10.1074/jbc.RA119.010565
- 73. Park JM, Harrison CE, Ma JJ, et al. Hyperpolarized C-13 MR spectroscopy depicts in vivo effect of exercise on pyruvate metabolism in human skeletal muscle. *Radiology*. 2021;300(3):626-632. doi:10.1148/radiol.2021204500

#### SUPPORTING INFORMATION

Additional supporting information can be found online in the Supporting Information section at the end of this article.

How to cite this article: Shaul D, Lev-Cohain N, Sapir G, et al. Real-time influence of intracellular acidification and  $Na^+/H^+$  exchanger inhibition on in-cell pyruvate metabolism in the perfused mouse heart: A  $^{31}$ P-NMR and hyperpolarized  $^{13}$ C-NMR study. *NMR in Biomedicine*. 2023;36(10):e4993. doi:10.1002/nbm.4993